Adsorption 11: 679–684, 2005

Growth Mode of Hydrogen in Mesoporous MCM-41. Adsorption and Neutron Scattering Coupled Studies

NICOLE FLOQUET* AND JEAN PAUL COULOMB
C.R.M.C.N - CNRS, Campus de Luminy, Case 901, 13288 Marseille Cedex 9, France
floquet@crmcn.univ-mrs.fr

PHILIPPE LLEWELLYN
MADIREL - UMR 6121, Centre de S^t Jérome, 13397 Marseille Cedex 20, France

GILLES ANDRE AND REMI KAHN
Laboratoire Léon - Brillouin, CEA - Saclay, 91191 Gif - sur - Yvette, Saclay, France

Abstract. X-ray or neutron diffractograms of calcined MCM-41 samples are strongly modified during the sorption phenomenon. Intensity of the main (100) peak (I_{100}) could undergo a non monotonous behaviour. At the sorption beginning I_{100} increases and I_{100} strongly decreases in the medium and high loading regimes. These observed intensity modifications in the diffractograms are closely related to the MCM-41 sample and to the filling mechanisms of its porosity. Actually each synthesis produces MCM-41 sample with its own silica wall and porosity. Several MCM-41 structural models and adsorption filling modes were attempted to fit all the diffractograms recorded during the D_2 adsorption in a MCM-41 ($Ø = 25$ Å) sample at $T = 16.4$ K. Our data agree with a MCM-41 having low density silica walls (20% voids) that is rarely reported. Consequently, the D_2 adsorption mechanism is proved to be more defined: at the low relative adsorption pressure D_2 fills the wall voids and forms a layer on the rough wall surface. Then at the relative pressure of the capillary step, D_2 fills the whole free MCM-41 mesopores. Even the solid capillary phase does not grow layer by layer on the inner pore walls but is growing up along the pore axis.

Keywords: MCM-41, porous structure, neutron diffraction, hydrogen sorption, filling modes

1. Introduction

Two main growth types exist for adsorbed species on flat surfaces The layer by layer growth mode (when the adsorbate perfectly wets the substrate) and the bulk crystallite growth mode (for non wetting or partial wetting behaviour). As it is schematically represented in Fig. 1, the layer by layer growth mode on a curved substrate induces more and more stress in the adsorbed film when it thickens. Concerning cylindrical pores such as MCM-41 mesopores, some questions are arising : what is the growth mode of the capillary phase? Does it depends on its nature (solid, liquid or hypercritical fluid) ? Actually, above the capillary critical temperature T_{cc} the confined phase is an hypercritical fluid. Its pore filling mode is trivial, it consists in the densification of the homogeneous fluid phase. Below T_{cc}, when the confined phase is a liquid, the usual capillary condensation occurs. But when the confined phase is a solid, does the capillary solid grow on the mesopore wall by a layer by layer mode or grow up along the mesopore axis as represented in Fig. 2.

From a quite simple comparison of adsorption isotherms, the last filling mode seems to prevail in the case of confined krypton in MCM-41 ($Ø = 40$ Å) at $T = 77.4$ K. Actually neutron diffraction experiments

*To whom correspondence should be addressed.

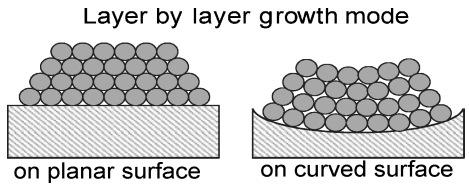

Figure 1. Schematic representation of the layer by layer growth mode on a planar surface and on a curved surface respectively.

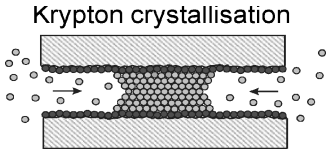

Figure 2. Schematic representation of the capillary solid growth of krypton in a cylindrical mesopore.

have pointed out that the krypton confined phase in MCM-41 (Ø = 40 Å) freezes at $T = 85$ K (Coulomb et al., 1998), thus it is a solid phase at $T = 77.4$ K. Adsorption isotherms of krypton on MCM-41 (Ø = 40 Å) and on graphite (Thomy and Duval, 1969) measured at the same temperature $T = 77.4$ K are represented in Fig. 3. The stepped shape isotherm (type-VI) of the krypton/graphite system is an illustration of the layer by layer growth mode. Each step represents the physisorption of a Kr monolayer (when the Kr film thickens the influence of the graphite substrate decreases strongly, as a consequence, the steps are closer and closer to the saturated vapor pressure P_0 of the bulk sorbate). Instead of a stepped isotherm, the confined solid krypton in MCM-41 (Ø = 40 Å) gives rise to a type-IV adsorption isotherm. Then, such signature of a solid capillary growth mode is rather a growth along the mesopore axis. The aim of the present paper is to show how an

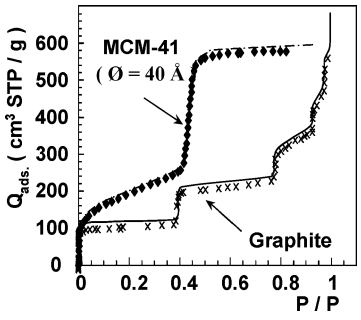

Figure 3. Sorption isotherms of krypton at $T = 16.4$ K on MCM-41 (Ø = 40 Å) and graphite.

accurate analysis of the MCM-41 diffraction patterns recorded during the isotherm adsorption is a way to characterize precisely the confined phase growth mode and consequently the porous structure of the MCM-41 samples. The reported study deals with deuterium adsorption in MCM-41 (Ø = 25 Å), this system being more appropriate to analyse the growth modes of the confined phase.

2. Experimental Section

The neutron diffraction experiment has been performed at the laboratory Léon Brillouin (C.E.A. - Saclay) on the G4-1 diffractometer. The MCM-41 (Ø = 25 Å) sample used was synthesized at the laboratory of K.K. Unger (Mainz-Germany). Prior to the experiment it was outgazed at $T = 573$ K under vacuum ($P < 10^{-6}$ torr) during around 12 hours. Fourteen diffractograms have been measured at different loadings for deuterated hydrogen confined phase in MCM-41 (Ø = 25 Å) at $T = 16.4$ K. A calibration sorption isotherm is measured during the neutron diffraction experiment.

3. Results and Discussion

Sorption isotherms on MCM-41 samples are composed of two parts that have common interpretation. In the low relative pressure regime ($P/P_0 \leq 0.1$) the isotherm shape looks like the usual type-I Langmuir isotherm (P_0 is the saturated vapor pressure of the bulk sorbate). Such a part corresponds to the film physisorption on the mesopore inner surface. The second part is characterized by a step formation due to the capillary condensation in the high relative pressure range $P/P_0 > 0.1$. The shape and the relative extension of the two parts greatly depend on the host porous material and on the considered confined species, as represented in Fig. 4 (Llewellyn et al., 1994; Coulomb et al., 1997). Deuterium sorbate was chosen because the two parts of the adsorption isotherm are equally developed.

Neutron diffractograms recorded during the isotherm adsorption prove the influence of the sorption phenomenon on the diffractograms of empty MCM-41 samples. Strong intensity modifications of the diffracted peaks are related to the two sorption isotherm parts previously described. Note that such modifications do not depend on the nature of both the physisorbed film or the capillary phase (solid, liquid or hypercritical fluid) (Marler et al., 1996; Coulomb

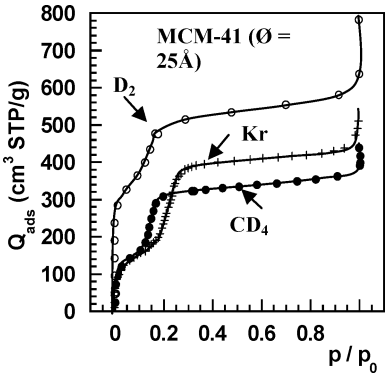

Figure 4. Sorption isotherms of D_2 (○) at $T = 16.4$ K, CD_4 (●) and Kr (+) on MCM- 41 (Ø = 25 Å) at $T = 77.4$ K.

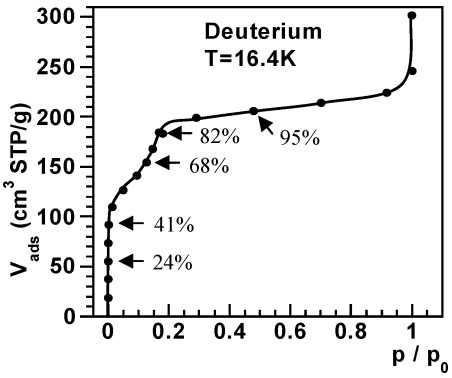

Figure 6. Deuterium adsorption isotherm on MCM-41 (Ø = 25 Å) measured at $T = 16.4$ K.

et al., 1997, 1998). The same intensity behaviour was observed for all the sorbate species that we have already studied (Coulomb et al., 1997, 1998) Futher, intensity increase is shown to depend on the MCM-41 pore diameter Ø and on the extension of the first isotherm part. Thus it appears that intensity modifications are closely related to the mechanisms of the MCM-41 mesopores filling. Actually, interference effects between the MCM-41 wall atoms (SiO_2) and the sorbate species (D_2) should modify the diffractogram of the empty MCM-41 sample. Such interference effects can be constructive or destructive depending of the sorbate position in the mesopore and the (hkl) diffraction peak. Recall that the same phenomenon has been usually observed during the sorption in zeolites (Coulomb et al., 1994, 1999; Floquet et al., 2003).

The neutron diffractograms plotted in Fig. 5 were measured during the sorption of D_2 at $T = 16.4$ K.

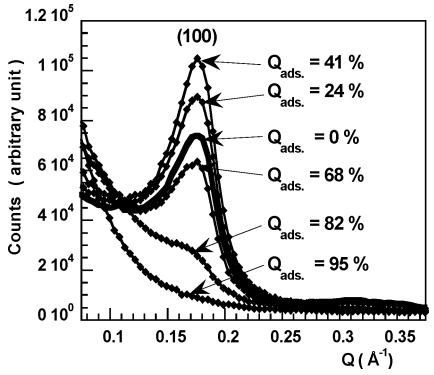

Figure 5. Neutron patterns of MCM-41 (Ø = 25 Å) at = 16.4 K as a function of D_2 loading.

Neutron diffractogram of the empty MCM-41 has one intense (100) peak and several weak (hk0) peaks characterizing the hexagonal network of pores. Spectacular effects on the intensity of the (100) peak is observed during the D_2 isotherm adsorption given in Fig. 6. There is an increase of the (100) peak intensity I_{100} up to a D_2 loading of 41%, in the first stage of the pore filling. In the case of idealised model of MCM-41 (hexagonal mesopores, amorphous silica wall with density of 2.2 g·cm^{-3}), it could be related to a layer by layer growth mode of D_2 film physisorbed to the inner wall of the MCM-41 mesopores. Indeed a layer by layer filling mode produces an increase of the MCM-41 wall thickness. As a consequence it could be expected associated to an intensity increase. Then, I_{100} is monotonously decreasing in the second stage of the pore filling which is generally related to the so called "capillary condensation" filling mode. I_{100} vanishes completely at high loading. A continuous intensity decrease is observed for the weak (110) and (200) peaks.

3.1. Filling Mode Modelling in MCM-41 Idealised Structure

To validate this usual scenario of the two filling modes, the first attempt was a modelling of the diffraction patterns similar to the one developed by Hammond et al. (1999). Their purpose was to interpret the change in Bragg X-ray scattering due to the MCM-41 template removal. Both the MCM-41 wall atoms and the sorbate atoms are supposed to be located on a discrete hexagonal lattice. The MCM-41 hexagonal pores are defined by the pore diameter Ø (Å) and the pore wall

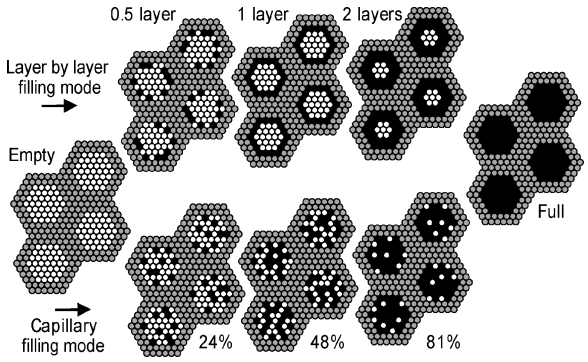

Figure 7. Illustration of the two filling modes of the MCM-41 mesopores used for the modelling of the diffracted (100) intensity.

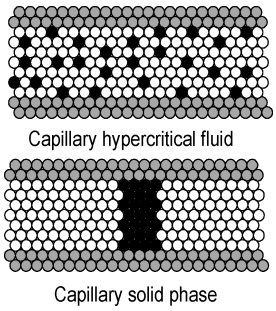

Figure 8. Illustration of two capillary phases in MCM-41 used for the modelling of the diffracted (100) intensity.

thickness t_w (Å). The unit cell parameter of the hexagonal pore network is $a_h = Ø + t_w$. Thus the hexagonal cross section of the pores is $S_{pore} = \sqrt{3}Ø^2/2$. Usual diffraction peak intensity I_{hkl} is calculated for different atomic sorbate positions and different sorbate loadings as schematically displayed in Fig. 7. The diffracted intensity I_{hkl} for a (hkl) reflection is related to the structure factor F_{hkl}, which is a complex quantity computed from atomic coordinates, atom form factors and temperature factors (F^*_{hkl} is the F_{hkl} complex conjugate). $I_{hkl} \cong F_{hkl} \cdot F^*_{hkl}$. The value of the structure factor F_{hkl} depends on the amount of the sorbate species and its location within the pore. Each structure factor F_{hkl} has two components, one related to the atoms (SiO_2) of the wall (F_w) and one related to the sorbate atoms located within the pore (F_s). Thus the structure factor is $F_{hkl} = F_w + F_s$ and the observed intensity is proportional to the quantity $(F_w + F_s) \cdot (F_w + F_s)^*$: $I_{hkl} = I_{hkl(W+S)} \cong F_w \cdot F^*_w + F_w \cdot F^*_s + F^*_w \cdot F_s + F_s \cdot F^*_s$. In the limit case where the pore diameter tends to zero ($Ø = 0$), only the amorphous silica gives rise to a broad diffraction bump in the high Q range. There are no more diffraction peaks characterizing the hexagonal network of the pores when there are no more pores. Then, $I_{hkl} = (F_w + F_p) \cdot (F_w + F_p)^* = 0$, if F_p is related to the SiO_2 atoms filling the pore. It follows that $F_w = -F_p$, then $I_{hkl} = (-F_p + F_s) \cdot (-F_p + F_s)^*$. For an empty pore $F_s = 0$, then $I_{hkl} = I_0 \cong F_p \cdot F^*_p$. It follows that the relative intensity I_r is expressed by $I_r = I_{hkl}/I_0 \cong l + (-F_p \cdot F^*_s - F^*_p \cdot F_s + F_s \cdot F^*_s)/(F_p \cdot F^*_p)$.

The modelling points out that, I_{100} calculated for both cases, capillary hypercritical fluid and capillary solid phase as represented in Fig. 8, is the same for a given loading. Further, the simulation outlines that intensity modifications depend both on the filling mode but also on the MCM-41 pore diameter Ø and wall thickness t_w. Thus, for a pore diameter $Ø < 2t_w$, I_{100} decreases continuously for both filling mode but the layer by layer D_2 loading produces a weaker intensity decrease than the capillary D_2 loading (see Fig. 9(a)). For a pore diameter $Ø > 2t_w$, I_{100} presents a non monotonous behaviour when increasing the layer by layer loading. I_{100} increases at the beginning of the layer by layer filling mode (see Fig. 9(b) and (c)). Thus, our conclusion is that our experimental diffraction data would fit with a MCM-41 having a pore diameter $Ø > 2t_w$ (or $Ø > 2a_h/3$) and a filling mode starting by a layer by layer adsorption.

In this idealised structural description of MCM-41, the quantity of adsorbed D_2 at $Q_{ads.} = 100\%$ corresponds to a pore diameter $Ø = 30$ Å. Figure 10 compares the experimental and the computed intensity I_r of the (100) peak corresponding to the two filling modes of MCM-41 hexagonal pores having a wall density $d_{SiO_2} = 2.2$ g·cm^{-3}. The modelling would not be satisfying. The computed intensity for a layer by layer mode has its maximum at $Q_{ads.} = 43\%$, but it is 30% lower than the experimental one. There is two ways in this modelling to increase the calculated intensity. The first way is an increase of the pore size, but it would not to correspond to the experimental adsorbed quantity. The second way is a decrease of the silica density of the walls. Actually a best fit was obtained for a pore diameter $Ø = 30$ Å, a wall thickness $t_w = 10$ Å and a density of the walls $d_{SiO_2} = 1.62$ g·cm^{-3}. The calculated intensity is shown in Fig. 11. The layer by layer mode ends at $Q_{ads.} = 43\%$, it corresponds to a D_2 film thickness $t_{film} = 1.25$ layer. Then starts the capillary filling mode up to the full loading. A misfit between the calculated and experimental data well appears during the first adsorption stage. The

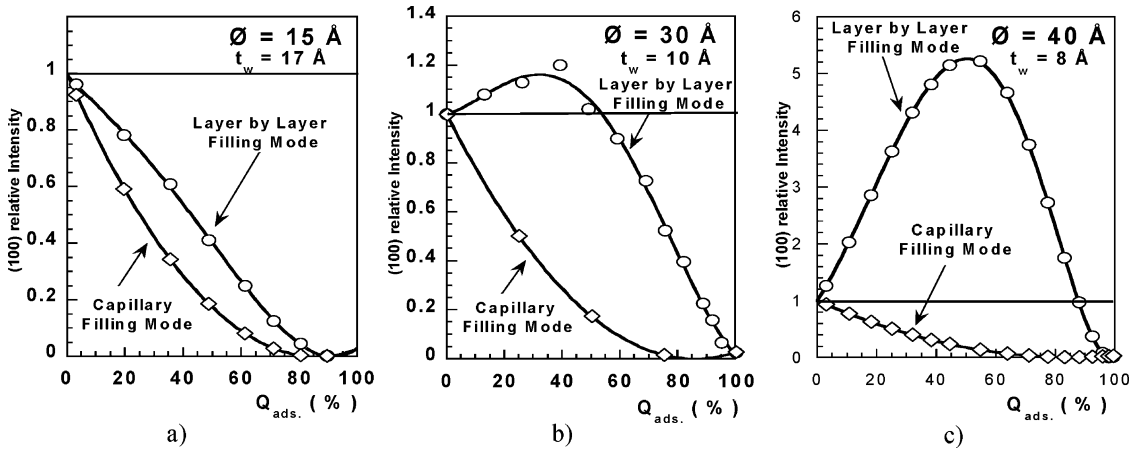

Figure 9. Calculated relative intensity I_r of the MCM-41 (100) peak as function of D_2 loading in the two filling modes, the layer by layer mode and the capillary mode, the density of the walls is $d_{SiO_2} = 2.2$ g·cm^{-3}, MCM-41 pore diameter (Ø) and wall thickness (t_w) are either with $Ø < 2t_w (Ø < 2a_h/3)$ in the case a or with $Ø > 2t_w (Ø > 2a_h/3)$ in the case b and c.

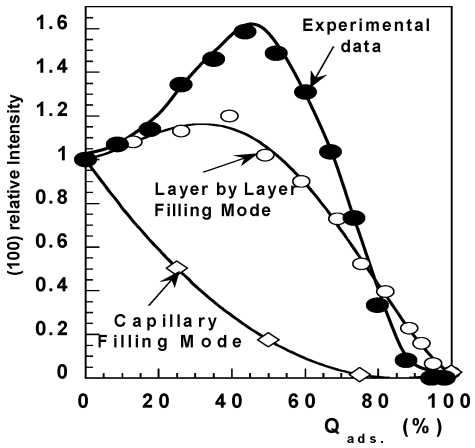

Figure 10. Experimental (●) and calculated relative intensity I_r of the MCM-41 (100) peak as function of D_2 loading in the two filling modes, the layer by layer mode and the capillary mode, case of a MCM-41 pore with diameter Ø = 30 Å and a density of the walls $d_{SiO_2} = 2.2$ g·cm^{-3}.

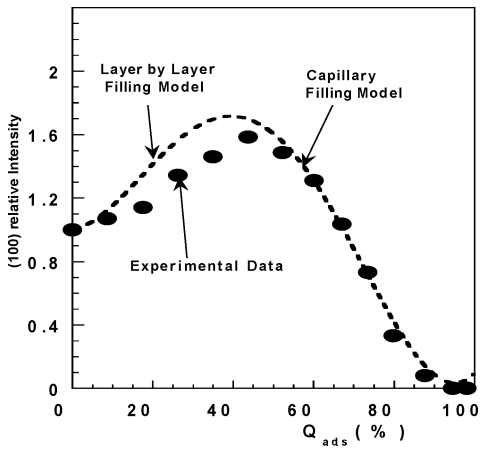

Figure 11. Experimental (●) and calculated (dashed line) relative intensity I_r of the MCM-41 (100) peak as function of D_2 loading. Successive filling mode modelling, the layer by layer mode up to 43%, then the capillary mode up to full loading; case of a MCM-41 pore diameter Ø = 30 Å and a density of the walls $d_{SiO_2} = 1.62$ g·cm^{-3}.

calculated intensity is larger than the experimental one. It means that the decrease of the silica density from 2.2 g·cm^{-3} to 1.6 g·cm^{-3} could be micropores inside the walls and that deuterium adsorbs this wall microporosity at the beginning of the adsorption. Such findings are not unexpected, a previous work (Edler et al., 1997) on structure and dynamics of hydrogen sorption in MCM-41 led to similar conclusions. Furthermore, other results (Floquet et al., 2004) from our structural analysis using the Rietveld method confirm these findings.

4. Conclusion

An accurate analysis of experimental diffractograms recorded during the adsorption is a successful way both to give detailed structural data of the porous structure of the MCM-41 sample and to characterize the growth mode of the adsorbed species in the MCM-41 sample. Actually from a simple structural modelling, it appears that, in the case of adsorption of most gas, an initial increase of the diffracted intensity of the first

intense (100) peak gives information on the pore diameter Ø and or the roughness and microporosity of the walls. It means that there is gas adsorption in the MCM-41 region r and $a_h/3 < r < (1 - a_h/3)$. Consequently, it means either that there is physisorption of a t_{film} thickness film on the inner MCM-41 walls and $(Ø - 2t_{film}) > 2a_h/3$, and or there is microporosity within the MCM-41 wall, and adsorption occurs in the MCM-41 wall porosity. Such experimental data could be obtained in most cases and would help greatly to the adsorption phenomenon analysis.

We plan now to study in details the hysteresis loop which characterizes the capillary condensation phenomenon. Such hysteresis loop (H-1 type) is known to be related to the meniscus shape which is different for the sorption branch (cylindrical meniscus) and for the desorption branch (spherical meniscus).

References

Coulomb, J.P., C. Martin, Y. Grillet, and N. Tosi-Pellenq, "Structural Analysis by Neutron Diffraction of Simple Gases (H_2, Ar, CH_4 and CF_4) Sorbed Phases in $AlPO_4$-5," in *Zeolites and Related Microporous Materials: State of the Art 1994*, J. Weitkamp et al. (Eds.), pp. 445–452, Elsevier Science Publishers B.V., Amsterdam, 1994.

Coulomb, J.P., C. Martin, Y. Grillet, P. Llewellyn, and G. André, "Structural Property of Methane (CD_4) and Hydrogen (D_2) Sorbed Phases on MCM-41 (Ø = 25 Å)," *Studies in Surface Sciences and Catalysis*, **105**, 1827–1834 (1997).

Coulomb, J.P., C. Martin, Y. Grillet, P.L. Llewellyn, and G. André, "Structural Properties of Simple Sorbed Gases (N_2, Kr, D_2O) Confined in MCM-41 Sample (Ø = 40 Å)," *Studies in Surface Science and Catalysis*, **117**, 309–316 (1998).

Coulomb, J.P., Y. Grillet, P. Llewellyn, C. Martin, and G. André, "Structural Properties of Krypton Confined in MCM-41 (Ø = 40 Å)," in *Fundam. of Adsorption VI*, F. Meunier (Ed.), pp. 147–152, Elsevier, 1998.

Coulomb, J.P., C. Martin, N. Floquet , P.L. Llewellyn, and Y. Grillet, "Structural Analysis of Methane Sorbed Phases on Silicalite-1, Mordenite, $AlPO_4$-5 and $AlPO_4$-11," in *12th International Zeolite Conference*, M.J. Treacy et al. (Eds.), pp. 197–202, MRS, Baltimore, 1999.

Coulomb, J.P., N. Floquet, Y. Grillet, P.L. Llewellyn, R. Kahn, and G. André, "Dynamic and Structural Properties of Confined Phases (Hydrogen, Methane and Water) in MCM-41 Samples (19 Å, 25 Å and 40 Å)," *Studies in Surface Science and Catalysis*, **128**, 235–242 (2000).

Edler, K.J., P.A. Reynolds, P.J. Branton, F.R. Trouw, and J.W. White, "Structure and Dynamics of Hydrogen Sorption in Mesoporous MCM-41," *J. Chem. Soc., Faraday Trans.,* **93**, 1667– 1674 (1997).

Edler, K.J., P.A. Reynolds, J.W. White, and D. Cookson, "Diffuse Wall Structure and Narrow Mesopores in Highly Crystalline MCM-41 Materials Studied by X-ray Diffraction," *J. Chem. Soc., Faraday Trans.,* **93,** 199–202 (1997).

Floquet, N., J.P. Coulomb, G. Weber, O. Bertrand, and J.P. Bellat, "Structural Signatures of type IV Isotherm Steps: Sorption of Trichloroethene, Tetrachloroethene and Benzene in Silicalite-I," *J. Phys. Chem. B*, **107**, 685–693 (2003).

Floquet, N., J.P. Coulomb, and G. André, "Hydrogen Sorption in MCM-41 by Neutron Diffraction Study. Characterization of the Porous Structure of MCM-41 and the Growth Mode of the Hydrogen Confined Phases," *Microporous and Mesoporous Materials*, **72**, 143–152 (2004).

Hammond, W., E. Prouzet, S.D. Mahanti, and T.J. Pinnavaia, "Structure Factor for the Periodic Walls of Mesoporous MCM-41 Molecular Sieves," *Microporous and Mesoporous Materials*, **27**, 19–25 (1999).

Llewellyn, P.L., Y. Grillet, F. Schüth, H. Reichert, and K.K. Unger, "Effect of Pore Size on Adsorbate Condensation and Hysteresis Within a Potential Model Adsorbent: M41S," *Microporous Mater.*, **3**, 345–349 (1994).

Marler, B., U. Oberhagemann, S. Vortmann, and H. Gies, "Influence of the Sorbate Type on the XRD Peak Intensities of Loaded MCM-41," *Microporous Materials*, **6**, 375–383 (1996).

Thomy, A. and X. Duval, "Adsorption of Simple Molecules on Graphite. I. Homogeneity of the Surface of of Exfoliated Graphite. Originality and Complexity of Adsorption Isotherms," *J. Chimie Physique et de Physico Chimie Biologique*, **66**, 1966–1973 (1969).